

Adaptive image watermarking using bidimensional empirical mode decomposition

Mohammed Arrazaki¹, Abdelouahed Sabri², Mohamed Zohry¹, Tarek Zougari³

¹Department of Mathematics, Faculty of Sciences, University AbdelMalek Essaadi, Tetouan, Morocco

²Department of Computer Science, Faculty of Sciences, University Sidi Mohamed Ben Abdellah, Fez, Morocco

³Department of Mathematics and Computer Science, National School of Applied Sciences, University AbdelMalek Essaadi, Tangier, Morocco

Article Info

Article history:

Received Sep 1, 2022

Revised Jan 29, 2023

Accepted Mar 8, 2023

Keywords:

Bidimensional empirical mode decomposition

Patchwork algorithm

Robustness

ABSTRACT

Digital watermarking is considered one of the technological means used to guarantee the security and authenticity of data transmitted over communication systems. A new method of image watermarking using the bidimensional empirical mode decomposition (BEMD) will be presented in this article, where the new idea is to use the BEMD of both the cover image and the watermark image. The embedding process consists of adding to each intrinsic modal function (IMF) of the cover image the corresponding IMF of the watermark image. The watermarked image contains three different watermarks and appropriate frequencies, which makes it more robust. We use this method for two reasons: first, to conserve the constituent characteristics of each IMF and second, to ensure the invisibility of the watermark. The results obtained showed a good response against different kinds of attacks. This technique has been compared with other methods of image watermarking based on decomposition BEMD, which showed good results.

This is an open access article under the [CC BY-SA](#) license.



Corresponding Author:

Mohammed Arrazaki

Department of Mathematics, Faculty of Sciences, University AbdelMalek Essaadi

Tetouan, Morocco

Email: rezaki_mohamed@hotmail.com

1. INTRODUCTION

The advancement of media documents and the practice of sharing them over the internet further increase the accessibility and the illegal distribution of multimedia data. In this context, digital watermarking is a robust technique protecting this data [1], [2]. We study two aspects of the digital watermarking process: embedding and detection. The watermark is said to be robust if it is detectable when the quality of the image is not deficient [3]. The watermark scheme is private (not blind) if it uses the cover image in the detection phase or public (blind) in the other case. A portrayal of different watermarking techniques can be explored in [4]–[8]. An image watermarking method is effective if it satisfies the conditions of perceptibility, robustness and capacity. The influence of the capacity on the robustness and the perceptibility should be taken into consideration [9]. Among the issues of image watermarking is how the technique shows more robustness against various attacks, without affecting the two factors perceptibility and capacity [9]. The image watermarking using bidimensional empirical mode decomposition (BEMD) was introduced in [10]. In general, these methods use the first intrinsic modal function (IMF) that contain the high frequencies to insert the watermark [11]–[14]. Additionally, these methods are more robust than other methods against different kinds of attacks, notably noise attacks and JPEG

compression, but they have some difficulties in terms of robustness against geometric attacks [15].

In this context, we suggest a new method of image watermarking based on BEMD. This method has shown good results for robustness against a variety of attacks. It has also proven its effectiveness in comparison to two other BEMD-based image watermarking techniques. In this article, we will explain an image watermarking method that is based on decomposing the cover image into three frequency ranges or IMFs (high, medium, and low frequency) using the BEMD and inserting a suitable frequency watermark at each frequency range. Moreover, the advantages of this method allow us to increase the capacity of the watermark without a noticeable influence on the robustness and the perceptibility of the watermarked image, which we will see in the experimental results.

2. EMPIRICAL MODE DECOMPOSITION OF 2D

Huang, in the late nineties, introduced a new method for signal processing that was more adaptive to non-stationary and non-linear signals called empirical mode decomposition (EMD) [16]. Research by Nunes *et al.* [17] in 2003 it was first applied in the field of image processing. This decomposition makes possible the extraction of structures at different scales and frequencies, including amplitude and frequency modulations. The principle of the BEMD is to develop each signal s into a set of functions by the signal itself called bidimensional intrinsic mode functions (BIMFs) or 2D IMFs and a residue. This procedure is known as a sifting process. The reconstitution of the original signal is done without the loss or distortion of information. The properties of an IMF are the following [17]: i) each IMF has the same number of zero crossings and extrema and ii) each IMF is symmetric with respect to the local mean. The BEMD method consists of the following steps [18]:

a. Initialize $r_0 = m$ (the residual) and $k = 1$ (the index number of IMF).

b. Extract the k^{th} IMF (sifting process):

i. Initialize $h_0 = r_{k-1}$ and $j = 1$.

ii. $j=1$ extract the local minima and maxima of h_{j-1} .

iii. Compute the upper envelope and lower envelope functions x_{j-1} and y_{j-1} by interpolating, respectively, the local minima and local maxima of h_{j-1} .

iv. Compute the mean envelope:

$$m_{j-1} = (x_{j-1} + y_{j-1})/2 \quad (1)$$

v. Update $h_j = h_{j-1} - m_{j-1}$ and $j = j + 1$.

vi. Calculate the stopping criterion:

$$SD(j) = \frac{1}{M \times N} \sum_{m=1}^M \sum_{t=0}^T \frac{(h_{j-1} - h_j)^2}{h_{j-1}^2 + \epsilon} \quad (2)$$

where ϵ is a (weak) term eliminating any divisions by zero.

g. Decision: repeat steps (ii) through (vi) until $SD_j < SD_{max}$ and then put $d_k = h_j$ (k^{th} IMF).

c. Update the residue $r_k = r_{k-1} - d_k$.

d. Repeat steps a-c with $k = k + 1$ until the number of extrema in r_k is less than 2.

3. METHOD

3.1. Watermark embedding

We use Bender's algorithm "patchwork" [19]. Figure 1 present an additive watermark scheme was applied to each of the first three IMFs of the cover image I , where the watermark of the k^{th} IMF is a k^{th} IMF of the watermark image after it is divided by 255 to make the values of each IMF in the interval $[-1, 1]$ (each pixel in our cover image has a value between 0 and 255, but during the BEMD decomposition process these values shift to values between -255 and 255. To get it between -1 and 1 each value is divided by 255). This is done for two reasons: first, to conserve the constituent characteristics of each IMF and second, to ensure mark invisibility in the watermarked image. The embedding scheme of the watermark is in the following form:

- Step 1: extract the first three IMFs and residue by BEMD of the cover image I :

$$I = \sum_{k=1}^n IMF_k + residue \quad \text{with } n = 3 \quad (3)$$

- Step 2: extract the first three IMFs and residue by BEMD of the watermark image W , and divide each IMF by 255:

$$W = \sum_{k=1}^n IMF'_k + residue' \quad \text{with } n = 3 \quad (4)$$

$$W_k = \frac{IMF'_k}{255} \quad \text{with } k = 1, 2, 3 \quad (5)$$

Finally, each W_k keeps the same characteristics but contains smaller amplitudes than those of IMF'_k .

- Step 3: embed the corresponding watermark in each IMF of the cover image:

$$IMF_{W_k} = IMF_k + W_k \quad \text{with } k = 1, 2, 3 \quad (6)$$

- Step 4: the watermarked image is constructed by adding all the watermarked IMFs and the residue of the BEMD of the cover image:

$$I_W = \sum_{k=1}^n IMF_{W_k} + residue \quad \text{with } n = 3 \quad (7)$$

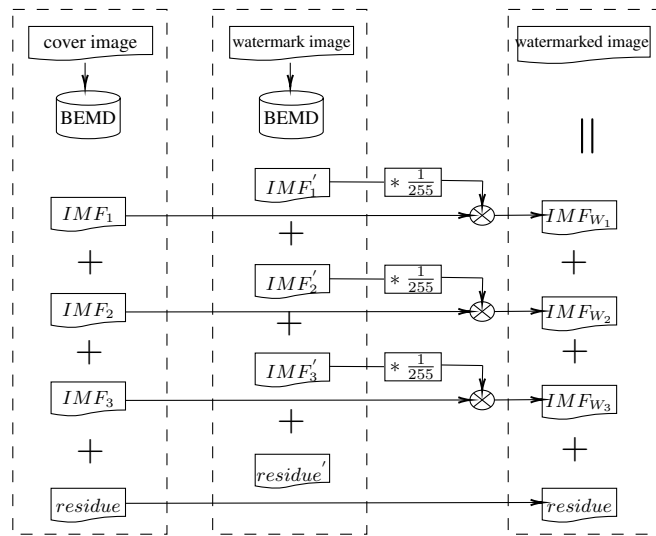


Figure 1. Diagram of watermark embedding process

3.2. Watermark extraction

We use the dual operation for watermark detection (Figure 2), explained in the following scheme:

- Step 1: extract the first three IMFs and residue by BEMD of the watermarked image I_W :

$$I = \sum_{k=1}^n IMF_{W_k} + residue \quad \text{with } n = 3 \quad (8)$$

- Step 2: extract the first three IMFs and residue by BEMD of the watermark image W , and divide each IMF by 255:

$$W = \sum_{k=1}^n IMF'_k + residue' \quad \text{with } n = 3 \quad (9)$$

$$W_k = \frac{IMF'_k}{255} \quad \text{with } k = 1, 2, 3 \quad (10)$$

- Step 3: extract three watermarks from the first three IMFs:

$$IMF_k^* = IMF_{W_k} - W_k \quad \text{with } k = 1, 2, 3 \quad (11)$$

$$I^* = \sum_{k=1}^n IMF_k^* + residue \quad \text{with } n = 3 \quad (12)$$

I^* is the recovered cover image from the watermarked image.

- Step 4: we can check for the presence of the watermark image by using the threshold and the correlation between each IMF_k^* and IMF_k and even between I and I^* .

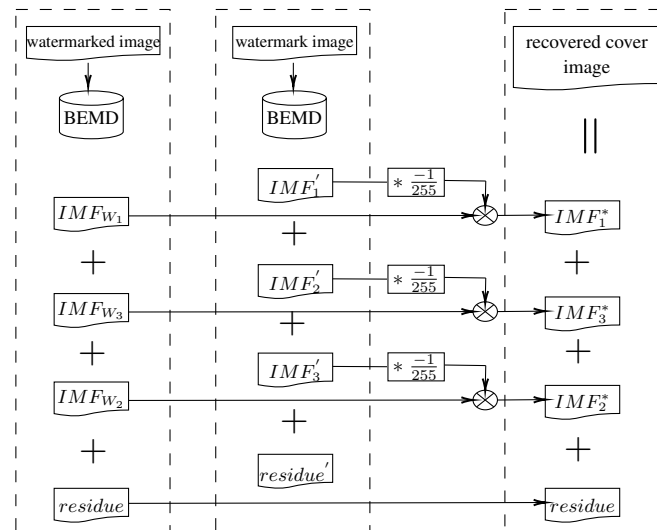


Figure 2. Diagram of watermark extraction process

4. RESULTS AND ANALYSIS

In Figure 3, we use a grayscale image (a cameraman (Figure 3(a)) as a simulation image for our watermarking method and a Moroccan Zellige image (Figure 3(b)) as a watermark. Both images are of equal size 255×255 . We have chosen to use the BEMD with compactly supported radial basis functions (BEMD-CSRBF) [20] in this algorithm instead of the classic BEMD [11].

4.1. Watermark embedding and extraction without attacks

Figure 3 presents a test of the invisibility characteristic that shows that it is well respected for our method, since the watermarked image (Figure 3(c)) has a good quality. Figure 4 shows the result of the extraction of the watermark image from the watermarked image (Figure 4(a)) without any attacks. Thus, a measurement of the correlation between the cover image and the recovered cover image from the watermarked image was used to check for the presence of the watermark image. Table 1 gives the correlation between the recovered cover image (Figure 4(b)) and the cover image (Figure 3(a)) and even the correlations between their IMFs. The results shown in Table 1 confirm that the watermark is easily detectable if there is no attack.

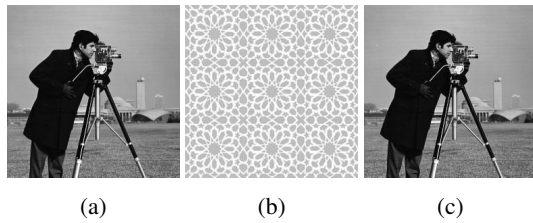


Figure 3. Watermark embedding: (a) cover image, (b) watermark image, and (c) watermarked image

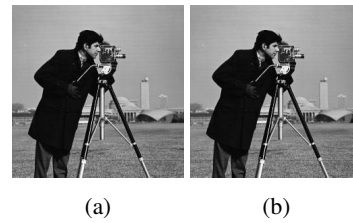


Figure 4. Watermark detection: (a) watermarked image and (b) recovered cover image

Table 1. Correlation

Images	IMF1s	IMF2s	IMF3s
1	0.9536	0.8822	0.8600

4.2. Robustness of the method in the presence of attacks

Once the watermarked images are broadcast on the internet. They might be the victims of attacks [21]–[23], either intentional or unintentional. Next, we present some examples of attacks/detection in order to test this method in terms of robustness.

4.2.1. Detection in the presence of white noise attacks

To test our method against Gaussian white additive noise, we will apply white noise of zero average and different variances to our watermarked image, we use the Wiener filter mask (5×5) to denoise our image (the watermarked image with white noise), which is assumed to be among the most effective lters against white noise attacks. Figure 5 shows the watermarked image under white noise attack with a variance of 0.1 (Figure 5(a)) and its denoising (Figure 5(b)). In Figure 6, the watermarked image under white noise attack with a 0.05 variance is presented in Figure 6(a) and its denoising is in Figure 6(b). Figure 7 shows the watermarked image attacked with white noise with a variance of 0.01 (Figure 7(a)) and its denoising (Figure 7(b)). Table 2 presents the correlations results for white noise with different variance values, which indicates that this method is resistant to this type of attack.

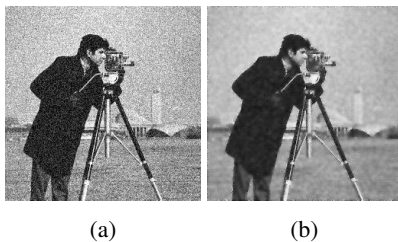


Figure 5. White noise var. 0.1: (a) watermarked image under white noise attack and (b) watermarked image after reducing the noise

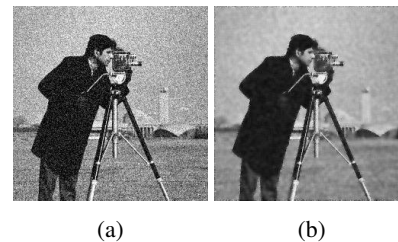


Figure 6. White noise var. 0.05: (a) watermarked image under white noise attack and (b) watermarked image after reducing the noise

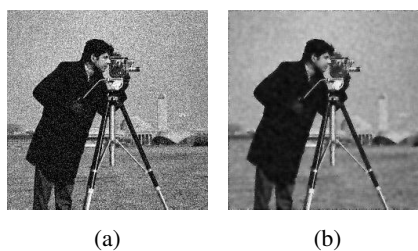


Figure 7. White noise var. 0.01: (a) watermarked image under white noise attack and (b) watermarked image after reducing the noise

Table 2. Correlation between cover image and each image (Figures 5(b), 6(b) and 7(b)) after extraction of the watermark

White noise variance	0.01	0.05	0.1
Correlation	0.9277	0.9276	0.9275

4.2.2. Detection in the presence of different kinds of attacks

In Table 3, we have tested our method in the presence of known attacks (rotation, median filter, Gaussian low-pass filter, (3×3) average filter, salt and pepper noise (0.001), JPEG compression with quality factor 50 (QF=50), JPEG2000 compression with compression ratio 12 (CR=12), motion blur (Theta=4 Len=7), sharpening (0.8), histogram equalization, and speckle noise (0.001)), we used different angles of rotation and different window size for the median filter. This table contains the results of the correlation between the cover image and the recovered cover image from the watermarked and attacked image. The correlation values obtained from all attacks tested are larger than 0.95, except the correlation of histogram equalization (0.93895). Moreover, the values corresponding to median filter remain stable with the change in window size, and likewise with small degree rotations. Therefore, from these results, we can see that our method is resistant against these attacks. In relation to the results achieved in the Table 3, we can observe in Figure 8, the quality of the recovered cover images under different attacks is not deficient. Which shows that the extraction process is generally done without problems. Figures 8(a)-(d), respectively, show the recovered cover image under rotation attacks with different degrees -0.5° , -0.25° , 0.25° , and 0.5° . The recovered cover images under median attacks are shown in Figure 8, median filter (3×3) (Figure 8(e)), median filter (5×5) (Figure 8(f)) and median filter (7×7) (Figure 8(g)). Figure 8 also shows the recovered cover images under the other attacks we mentioned earlier, Gaussian low-pass filter (Figure 8(h)), JPEG compression with quality factor 50 (Figure 8(i)), JPEG2000 compression with compression ratio 12 (Figure 8(j)), motion blur with Theta=4 and Len=7 (Figure 8(k)), sharpening 0.8 (Figure 8(l)), salt and pepper noise 0.001 (Figure 8(m)), histogram equalization (Figure 8(n)), speckle noise (0.001) (Figure 8(o)), and average filter (3×3) (Figure 8(p)).

Table 3. Correlation between the cover image and the recovered cover image

Attack		Correlation
Angle of rotation ($^\circ$)	-0.5	0.9998
	-0.25	0.9997
	0.25	0.9997
	0.5	0.9998
Median filter	3 * 3	0.9840
	5 * 5	0.9646
	7 * 7	0.9505
Gaussian low-pass filter	3 * 3	0.9976
JPEG compression	QF = 50	0.9943
JPEG2000 compression	CR = 12	0.9955
Motion blur	Theta = 4, Len = 7	0.9566
Sharpening	0.8	0.9917
Salt and pepper noise	0.001	0.9971
Histogram equalization		0.9389
Speckle noise	0.001	0.9976
Average filter	3 * 3	0.9790

4.2.3. Comparison with other watermarking algorithms using BEMD decomposition

In this section, our algorithm is compared with two approaches of image watermarking using BEMD, the first method based on the lifting wavelet transform (LWT) and the BEMD [24], the second method based on self-fractional fourier function (SFFF) and BEMD with cyclic error correction coding [25]. Table 4 shows the robustness of these methods against some attacks using the cover image of size 512×512 and the watermark image of size 256×256, knowing that the normalized correlation (NC) value is calculated between the watermark image and the recovered watermark image. The NCs values of (2×2) median filter, (3×3) Gaussian filter, and JPEG compression (10, 20, 30, 40, and 50) concerning our method are higher than those of [24]. Comparing with [25], we found that the NCs values of all previous attacks plus 3×3 median filter and (2×2) Gaussian filter are slightly improved. The robustness comparison showed in general that our algorithm has better NCs values compared to the others, which means that it is better robust against these attacks. According to this comparison with the two methods, we have seen how our method improved the robustness results of the

tested attacks, although the method [24] has already given significant results. This improvement comes from the adaptive approach used in the watermark embedding phase.

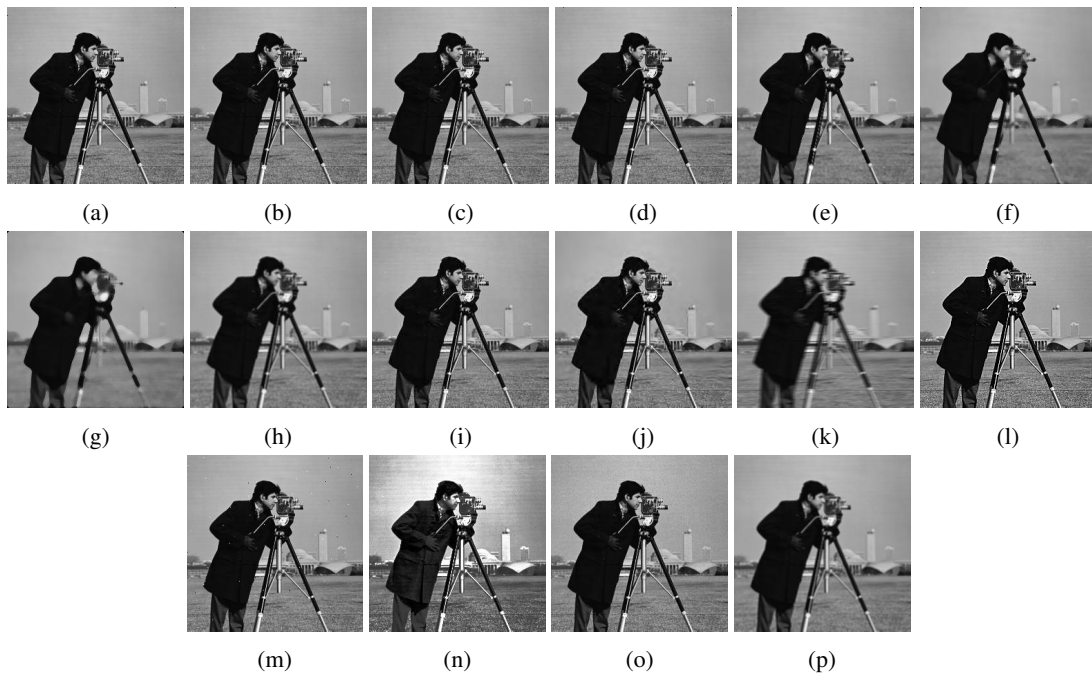


Figure 8. Recovered cover images (cameraman) from the watermarked and attacked images cameraman: (a) angle of rotation -0.5° , (b) angle of rotation -0.25° , (c) angle of rotation 0.25° , (d) angle of rotation 0.5° , (e) median filter 3×3 , (f) median filter 5×5 , (g) median filter 7×7 , (h) Gaussian low-pass filter, (i) JPEG compression $QF=50$, (j) JPEG2000 compression $CR=12$, (k) motion blur $\Theta=4$; $Len=7$, (l) sharpening 0.8, (m) salt and pepper noise 0.001, (n) histogram equalization, (o) speckle noise 0.001, and (p) average filter 3×3

Table 4. The NC results comparison with that in [24] and in [25], NaN design that the corresponding values are not available

Attack		[24]	[25]	Our method
Median filter	2×2	0.9950	NaN	0.99928
	3×3	0.9940	0.8760	0.99925
Gaussian filter	2×2	0.9950	NaN	0.99798
	3×3	0.9950	0.9590	0.99947
JPEG compression	$QF = 10$	0.9940	0.8360	0.99832
	$QF = 20$	0.9950	0.8456	0.99907
	$QF = 30$	0.9950	0.8757	0.99931
	$QF = 40$	0.9950	0.8816	0.99943
	$QF = 50$	0.9950	0.8904	0.99951
Speckle noise	0.1	0.9930	NaN	0.99950

5. CONCLUSION

A new method of image watermarking using BEMD is presented in this manuscript. The main idea is embedding the appropriate frequency watermark in each of the first three IMFs of the cover image (the watermarked image contains three different watermarks and suitable frequencies), which provides more robustness to the watermarked image. In the presence of different attacks, the robustness test results show a good response. Therefore, the comparison with other image watermarking methods using BEMD gave a better performance in terms of robustness for most of the attacks tested.




ACKNOWLEDGEMENT

We want to express our thanks to Pr. Adel BABBAH for his help in this work.




REFERENCES

- [1] V. S. Verma and R. K. Jha, "An overview of robust digital image watermarking," *IETE Technical Review*, vol. 32, no. 6, pp. 479–496, Nov. 2015, doi: 10.1080/02564602.2015.1042927.
- [2] H. Tao, L. Chongmin, J. M. Zain, and A. N. Abdalla, "Robust image watermarking theories and techniques: a review," *Journal of Applied Research and Technology*, vol. 12, no. 1, pp. 122–138, Feb. 2014, doi: 10.1016/S1665-6423(14)71612-8.
- [3] W. Wan, J. Wang, Y. Zhang, J. Li, H. Yu, and J. Sun, "A comprehensive survey on robust image watermarking," *Neurocomputing*, vol. 488, pp. 226–247, Jun. 2022, doi: 10.1016/j.neucom.2022.02.083.
- [4] S. Agreste and L. Puccio, "Wavelet-based watermarking algorithms: theory, applications and critical aspects," *International Journal of Computer Mathematics*, vol. 88, no. 9, pp. 1885–1895, Jun. 2011, doi: 10.1080/00207160.2010.502225.
- [5] M. U. Celik, G. Sharma, A. M. Tekalp, and E. Saber, "Lossless generalized-LSB data embedding," *IEEE Transactions on Image Processing*, vol. 14, no. 2, pp. 253–266, 2005, doi: 10.1109/TIP.2004.840686.
- [6] Z. Ni, Y.-Q. Shi, N. Ansari, and W. Su, "Reversible data hiding," *IEEE Transactions on Circuits and Systems for Video Technology*, vol. 16, no. 3, pp. 354–362, Mar. 2006, doi: 10.1109/TCSVT.2006.869964.
- [7] Z. Wenyin and F. Y. Shih, "Semi-fragile spatial watermarking based on local binary pattern operators," *Optics Communications*, vol. 284, no. 16–17, pp. 3904–3912, Aug. 2011, doi: 10.1016/j.optcom.2011.04.004.
- [8] C. Kumar, A. K. Singh, and P. Kumar, "A recent survey on image watermarking techniques and its application in e-governance," *Multimedia Tools and Applications*, vol. 77, no. 3, pp. 3597–3622, Feb. 2018, doi: 10.1007/s11042-017-5222-8.
- [9] S. M. Mousavi, A. Naghsh, and S. A. R. Abu-Bakar, "Watermarking techniques used in medical images: a survey," *Journal of Digital Imaging*, vol. 27, no. 6, pp. 714–729, Dec. 2014, doi: 10.1007/s10278-014-9700-5.
- [10] W. Huang and Y. Sun, "A new image watermarking algorithm using BEMD method," in *2007 International Conference on Communications, Circuits and Systems*, Jul. 2007, pp. 588–592, doi: 10.1109/ICCCAS.2007.4348123.
- [11] A. Sabri, M. Karoud, H. Tairi, and A. Aarab, "A robust image watermarking based on the empirical mode decomposition," *International Review on Computers and Software*, vol. 4, no. 3, pp. 8–13, 2009.
- [12] X. Wang, K. Hu, J. Hu, L. Du, A. T. S. Ho, and H. Qin, "Correction to: robust and blind image watermarking via circular embedding and bidimensional empirical mode decomposition," *The Visual Computer*, vol. 37, no. 4, pp. 859–859, Apr. 2021, doi: 10.1007/s00371-020-01948-9.
- [13] S. Kannadhasan and R. Suresh, "EMD algorithm for robust image watermarking," *Advanced Materials Research*, vol. 984–985, pp. 1255–1260, Jul. 2014, doi: 10.4028/www.scientific.net/AMR.984-985.1255.
- [14] Laxmanika and P. K. Singh, "Robust and imperceptible image watermarking technique based on SVD, DCT, BEMD and PSO in wavelet domain," *Multimedia Tools and Applications*, vol. 81, no. 16, pp. 22001–22026, Jul. 2022, doi: 10.1007/s11042-021-11246-8.
- [15] S. Amira-Biad, T. Bouden, M. Nibouche, and E. Elbasi, "A bi-dimensional empirical mode decomposition based watermarking scheme," *International Arab Journal of Information Technology*, vol. 12, no. 1, pp. 24–31, 2015.
- [16] N. E. Huang et al., "The empirical mode decomposition and the Hilbert spectrum for nonlinear and non-stationary time series analysis," *Proceedings of the Royal Society of London. Series A: Mathematical, Physical and Engineering Sciences*, vol. 454, no. 1971, pp. 903–995, Mar. 1998, doi: 10.1098/rspa.1998.0193.
- [17] J. C. Nunes, Y. Bouaoune, E. Delechelle, O. Niang, and P. Bunel, "Image analysis by bidimensional empirical mode decomposition," *Image and Vision Computing*, vol. 21, no. 12, pp. 1019–1026, Nov. 2003, doi: 10.1016/S0262-8856(03)00094-5.
- [18] A. Sabri, M. Karoud, H. Tairi, and A. Aarab, "Image watermarking using the empirical mode decomposition," in *5th International Conference: Sciences of Electronic, Technologies of Information and Telecommunications*, 2009, pp. 1–6.
- [19] W. Bender, D. Gruhl, N. Morimoto, and A. Lu, "Techniques for data hiding," *IBM Systems Journal*, vol. 35, no. 3-4, pp. 313–336, 1996, doi: 10.1147/sj.353.0313.
- [20] M. Arrazaki and T. Zougari, "L'utilisation de fonction radiale de base à support compact pour accélérer le temps de décomposition BEMD," *IOSR journal of VLSI and Signal Processing*, vol. 4, no. 3, pp. 24–29, 2014, doi: 10.9790/4200-04312429.
- [21] S. Voloshynovskiy, S. Pereira, T. Pun, J. J. Eggers, and J. K. Su, "Attacks on digital watermarks: classification, estimation based attacks, and benchmarks," *IEEE Communications Magazine*, vol. 39, no. 8, pp. 118–126, Aug. 2001, doi: 10.1109/35.940053.
- [22] F. Y. Shin, "Watermarking Attacks and Tools," in *Digital Watermarking and Steganography*, 2nd ed., Boca Raton, FL: CRC Press, 2017, pp. 51–63, doi: 10.1201/9781315219783-5.
- [23] C. Song, S. Sudirman, M. Merabti, and D. Llewellyn-Jones, "Analysis of digital image watermark attacks," in *2010 7th IEEE Consumer Communications and Networking Conference*, Jan. 2010, pp. 1–5, doi: 10.1109/CCNC.2010.5421631.
- [24] N. H. Abbas, S. M. S. Ahmad, S. Parveen, W. A. Wan, and A. R. bin Ramli, "Design of high performance copyright protection watermarking based on lifting wavelet transform and bi empirical mode decomposition," *Multimedia Tools and Applications*, vol. 77, no. 19, pp. 24593–24614, Oct. 2018, doi: 10.1007/s11042-017-5488-x.
- [25] J. B. Sharma, K. K. Sharma, and V. Sahula, "Digital image dual watermarking using self-fractional fourier functions, bivariate empirical mode decomposition and error correcting code," *Journal of Optics*, vol. 42, no. 3, pp. 214–227, Sep. 2013, doi: 10.1007/s12596-013-0125-1.




BIOGRAPHIES OF AUTHORS

Mohammed Arrazaki    received his Ph.D. degree in 2021 for his research work in applied mathematics from Faculty of Sciences Tetouan, Morocco. His fields of interest are image processing, image analysis, and applied mathematics. He can be contacted at email: rezaki_mohamed@hotmail.com.






My Abdelouahed Sabri    is a Professor at the Faculty of Sciences, Fez Morocco. He received his Ph.D. degree in 2009 from Faculty of Sciences, Fez Morocco. His research areas include image processing and information retrieval. He can be contacted at email: abdelouahed.sabri@gmail.com.



Mohamed Zohry    is a Professor at the Faculty of Sciences Tetouan Morocco. He received his PhD degree in 1983 from Faculty of Sciences, Rabat, Morocco. And Ph.D. in 1996 at Granada University (Spain). His research areas include analysis, geometry and topology, number theory, applied mathematics, statistics, and probability theory. He can be contacted at email: zohry@hotmail.fr.



Tarek Zougari    is currently a Professor in the ENSAT (National Schools of Applied Sciences of Tangier) at the Abdel Malek Essaadi University. He obtained his Ph.D. from the University of Poitiers Fr. with a specialization in control theory and applied mathematics. His fields of interest are image processing and number theory. He can be contacted at email: zougari123@gmail.com.